How to cite: *Angew. Chem. Int. Ed.* **2023**, *62*, e202305404
doi.org/10.1002/anie.202305404

Luminescence

Circularly Polarized Luminescence from Cyclic (Alkyl)(Amino) Carbene Derived Propellers

Jan Lorkowski, Dylan Bouetard, Patrick Yorkgitis, Milan Gembicky, Thierry Roisnel, Nicolas Vanthuyne, Dominik Munz,* Ludovic Favereau,* Guy Bertrand, Marc Mauduit,* and Rodolphe Jazzar**

In memory of Professor Jacek Gawroński

Abstract: Organic circularly polarized luminescence (CPL)-active molecular emitters featuring dynamic propeller-like luminophores were prepared in one step from cyclic(alkyl)(amino) carbenes (CAACs). These molecules exhibit through-space arene-arene π-delocalization and rapid intramolecular inter-system crossing (ISC) in line with their helical character.

The controlled manipulation of circularly polarized (CP) light is highly sought after in numerous fields of technology,[1] such as 3D displays,[2] sensors,[3] information storage,[4] spintronics,[5] and optoelectronic devices.[6] It is also essential in biology,[7] and was observed for dynamically chiral helical polymers, which function as enantioselective catalysts.[8] CP luminescence (CPL)—the differential emission of right- and left-CP light—is typically achieved using chiral luminophores.[9] Historically, chiral lanthanide complexes have been the class of choice for investigating CPL because of their high luminescence dissymmetry factors ($|g_{lum}|$) of up to 1.5.[1,10] Recently, despite lower $|g_{lum}|$ ($10^{-2} > |g_{lum}| > 10^{-4}$),[11] chiral organic molecules have attracted increasing attention thanks to their superior emission quantum yields (Φ), tunable photophysical properties, and straightforward integration into optoelectronic devices.[3,12] The vast majority of small organic emitters investigated so far, are derived from three scaffolds which display configurationally stable chirality, namely helicenes,[13] [2.2]paracyclophanes,[14] and binaphthyls[15] (Figure 1, top). Among them, carbohelicenes excel with remarkable chiroptical properties, in part owing to their extended helical π-conjugation and through-space π-delocalization.[16] In comparison, molecular propellers which represent another class of CPL emitters are mostly unexplored. Arguably, this is due to the difficulty of controlling the dynamics of their helically chiral conformations, which is critical for efficient through-space π-delocalization (Figure 1, middle).[17] To achieve this control, innovative synthetic approaches to original scaffolds are needed. Recently, cyclic (alkyl)-(amino)carbenes (CAACs),[18] which are highly ambiphilic singlet carbenes, emerged as attractive blocks for functional materials.[19] We envisioned that their concise and modular syntheses should give access to a novel class of CPL active molecular propellers via an intramolecular C–H insertion of the carbene carbon atom into the trityl C–H bond (Figure 1, bottom).[20]

This synthetic strategy is attractive for several reasons. First, it combines a trityl group—a privileged chiral "sensor"[21]—and a CAAC scaffold chiral "inducer".[22] Second, it capitalizes on the diversity of available CAAC precursors that enables seamless structural variations.[23] Lastly, the intramolecular C–H insertion step enforces close steric interactions. Overall, this approach allows for controlling the electronic and chiroptical properties, as well as material processability, by enabling rational engineering of

[*] Dr. J. Lorkowski, P. Yorkgitis, Dr. M. Gembicky, Prof. Dr. G. Bertrand, Dr. R. Jazzar
UCSD–CNRS Joint Research Laboratory (UMI 3555), Department of Chemistry and Biochemistry, University of California, San Diego
La Jolla, CA-92093-0343 (USA)
E-mail: jalorkowski@ucsd.edu
rjazzar@ucsd.edu

Dr. J. Lorkowski, D. Bouetard, Dr. T. Roisnel, Dr. M. Mauduit
Univ Rennes, Ecole Nationale Supérieure de Chimie de Rennes, CNRS, ISCR UMR 6226
35000 Rennes (France)
E-mail: marc.mauduit@ensc-rennes.fr

Dr. L. Favereau
Univ Rennes, CNRS, ISCR - UMR 6226
35000 Rennes (France)
E-mail: ludovic.favereau@univ-rennes1.fr

Prof. Dr. D. Munz
Coordination Chemistry, Saarland University, Campus C4.1
66123 Saarbrücken (Germany)
E-mail: dominik.munz@uni-saarland.de

Dr. N. Vanthuyne
Aix Marseille Univ., CNRS, Centrale Marseille, ISM2
13013 Marseille (France)

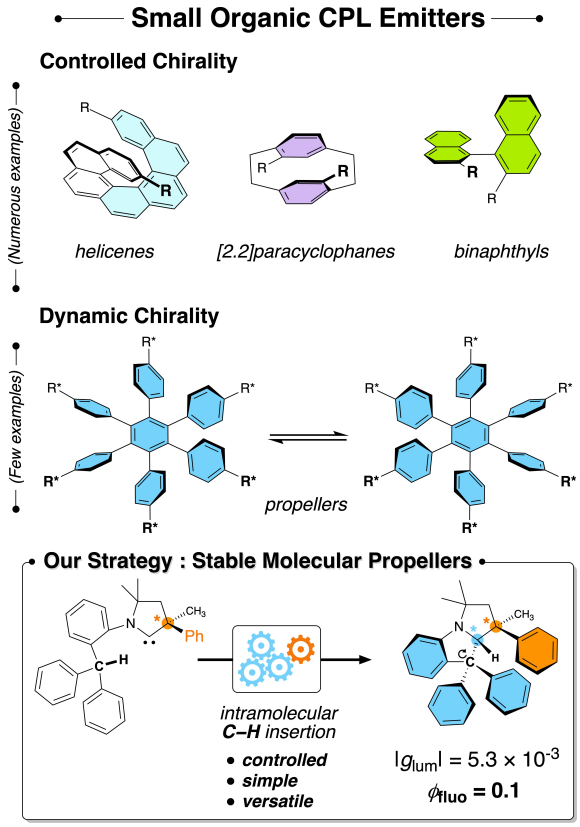

Figure 1. Overview of small organic CPL emitters vs. our strategy.

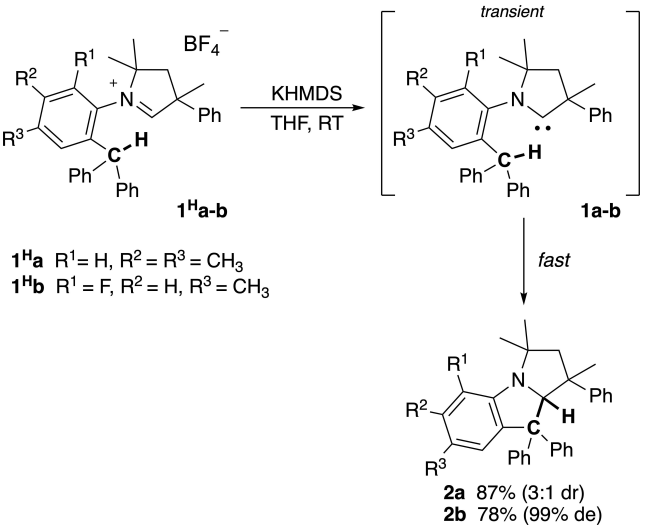

Scheme 1. Synthesis of racemic compounds **2a–b.**

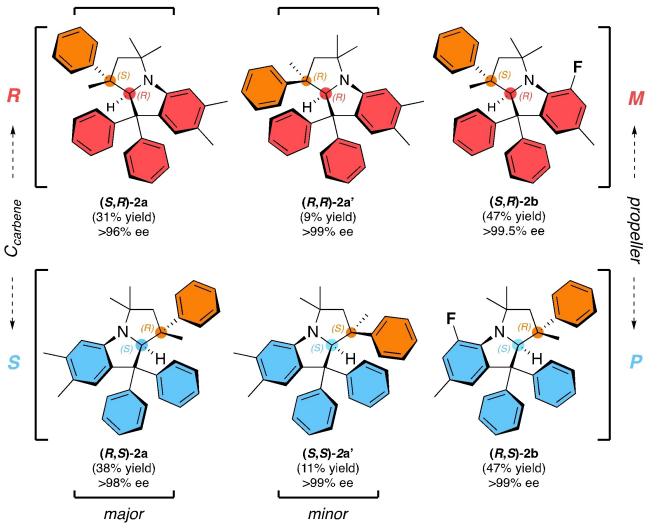

Figure 2. Enantiopure CAAC derived frameworks obtained by preparative chiral HPLC.

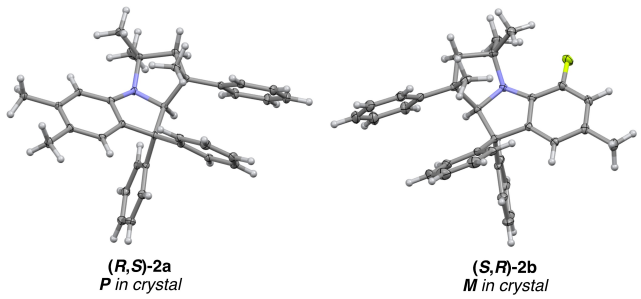

Figure 3. X-ray structure of compounds **(*R*,*S*)-2a** and **(*S*,*R*)-2b**.[26]

stereochemistry dense CAAC skeletons. Herein, we report the preparation and photophysical properties of propeller-type chiral CPL emitters derived from chiral singlet carbenes. Thanks to an efficient through-space π-delocalization, these simple trityl-carbene hybrids show $|g_{lum}|$ values as high as 5.3×10^{-3} and Φ of 0.1, which is on par with other state of the art structural motifs.

Synthesis. To begin, we prepared CAAC iminium salt **1a^{H}**, which is conveniently available in gram scale quantities.[23] As shown by us and others, the high ambiphilicity of CAACs permits intramolecular C–H activation at the carbene center.[19,20b] Indeed, deprotonation of **1a^{H}** with KHMDS led to subsequent carbene insertion into the acidic C–H bond of the trityl moiety forming compound **2a**, which was obtained in 87 % as a mixture of two diastereoisomers (3:1 dr, Scheme 1). Using the same strategy, we also obtained compound **2b** bearing *ortho* fluoro substituent (99 % de) on the pendant aniline moiety. Both products are bench-stable allowing for their easy separation under ambient conditions. Chiral-HPLC afforded the corresponding enantiomers in high enantiomeric excess (ee > 96 %, Figure 2). The absolute configuration of **(*R*,*S*)-2a** and **(*S*,*R*)-2b** was determined by SC-XRD (Figure 3), while the stereocenters of the minor diastereomers **2a′** were assigned by ECD (Electronic circular dichroism) spectroscopy.[24] Importantly, the trityl fragments in both structures display a chiral, propeller-like conformation, wherein the aryl rings adopt a *P* and *M*-type helical twist, respectively. The helicity was assigned by measuring the dihedral angles between the nearest C_{ipso} and C_{ortho} atoms. The values for **(*S*,*R*)-2b** in the

solid state ($\omega_1 = -78°$, $\omega_2 = 44°$ and $\omega_3 = 24°$, Table S1) indicate an M-type propeller.[21a]

Related three-blade propeller chirality has been previously studied by Mislow, Gawroński and others.[21] Examples of trityl- and triarylborane derivatives featuring dynamic three-fold symmetry remain limited.[25] Altogether, these observations suggest that the stereocenters on the CAAC scaffold allow for conformational control of the propeller associated with the trityl group.

Dynamic properties. To rationalize these observations, the conformational space of **2a**,**b** in solution was investigated by DFT calculations (r^2SCAN-3c, SMD = CH_2Cl_2), complemented by ab initio single points at the DLPNO-CCSD(T)//def2-TZVPP level of theory (Figure S16).[27] Of the three aryl groups present in the trityl moiety of ***(S,R)*-2b**, clockwise rotation of the equatorial trityl phenyl group gears with the phenyl substituent in axial position (Figure 4; for an animation, see Gif-S1). This process is associated with

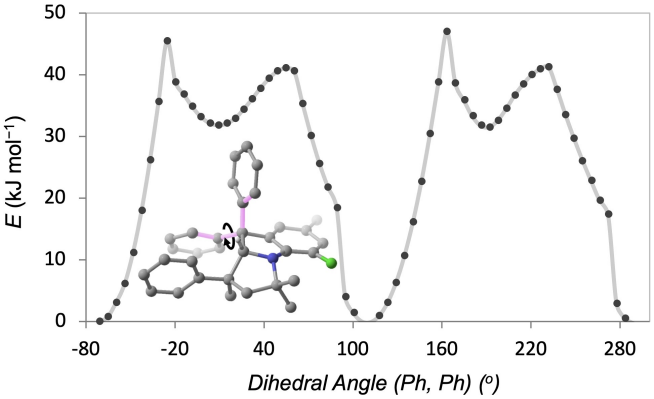

Figure 4. Gear behavior of ***(S,R)*-2b** upon clockwise rotation of the equatorial phenyl group (r^2SCAN-3c(SMD = CH_2Cl_2). For other rotational modes, see Figures S5–S9.

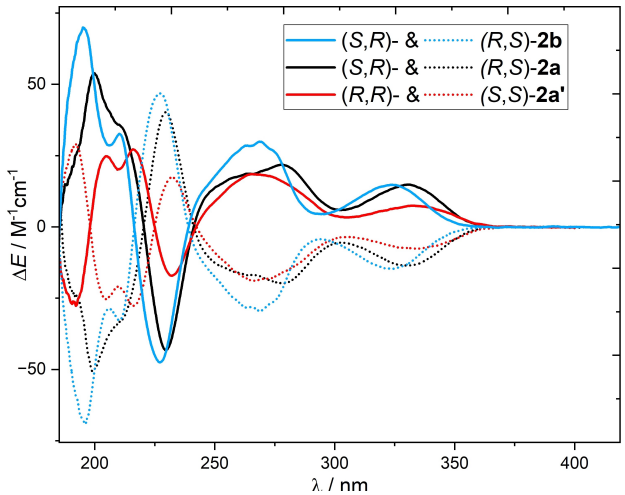

Figure 5. ECD spectra of ***(S,R)*-** and ***(R,S)*-2b** (solid and dotted blue lines, respectively), ***(S,R)*-** and ***(R,S)*-2a** (solid and dotted black lines, respectively) and ***(R,R)*-** and ***(S,S)*-2a′** (solid and dotted red lines, respectively) measured in acetonitrile ($\approx 10^{-5}$ M) at 298 K.

an overall barrier of $\Delta G^{\ddagger} = +47$ kJ mol^{-1} and, thus, proceeds swiftly at room temperature. Interestingly, counter-clockwise rotation (Figure S7) leads to gear-slippage and racemization via a two-ring flip pathway ($\Delta G^{\ddagger} = +42$ kJ mol^{-1}).[28] We thus conclude that the diastereotopic environment is efficiently sensed by the propeller, leading to a stabilization of one single conformer through residual stereoisomerism.

Ground-state photophysical and chiroptical properties. To further study the stereoinduction on the trityl propeller by the CAAC scaffold, we turned our attention to the photophysical and chiroptical properties. The UV/Vis spectrum of **2b** (Figure S4) was recorded in acetonitrile and reveals two low-energy bands of modest intensity at 260 and 323 nm ($\varepsilon \approx 1.2$ and 0.3×10^4 M^{-1}cm^{-1}, respectively). ECD measurements of enantiomers ***(R,S)*-2b** and ***(S,R)*-2b** display expected mirror-image spectra (Figure 5), which for ***(S,R)*-2b** include two positive transitions at 270 and 324 nm ($\Delta\varepsilon \approx 29$ and 15 M^{-1}cm^{-1}, respectively). Further, the strong positive Cotton effect observed at 210 nm is reminiscent of the characteristic ECD signals found for the triphenylmethyl group by Gawroński et al., which has been labeled a marker for this type of dynamic helicity.[21] These findings demonstrate that the preferred dynamic helical arrangement of the trityl group is in **2**-*M*-type configuration when the carbene carbon atom is *R*-configured (and vice-versa).[29] They support communication between the trityl group "sensor" and the CAAC scaffold "inducer" and rationalize the high absorption dissymmetry factor, g_{abs}, of 1.2×10^{-2} (at 330 nm), which is similar to the typical values observed with parent [6]helicene (g_{abs} 1.0×10^{-2}),[30] and other more sophisticated carbohelicenes (g_{abs} of 1.1×10^{-2}).[16]

To better understand the relevant electronic absorption spectra, further computational studies were performed (cam-B3LYP(CPCM = MeCN)/def2-TZVPP//r^2SCAN-3c). sTD-DFT[31] models for ***(S,R)*-2b** corroborate the experimental results, predicting a band of moderate intensity at 324 nm, and a stronger band at 269 nm (Figure S13; for ***(R,S)*-2a** and ***(R,R)*-2a′** see Figures S16, S17). The higher-energy ECD features are likewise reproduced, with a negative signal computed at 232 nm (S9 excited state) and a positive signal at 211 nm (S16 excited state). The S0→S1 transition may be approximated with a weight of 0.78 as the HOMO→LUMO transition (HOMO: Highest Occupied Molecular Orbital; LUMO: Lowest Unoccupied Molecular Orbital). Visual inspection of the molecular orbital (MO) isosurface plots reveals that the HOMO is localized on the fluorinated phenyl ring and the nitrogen atom of the CAAC (Figure 6). The LUMO also involves the fluorinated ring, yet strongly mixes with the π* of the adjacent trityl phenyl ring. This suggests intramolecular charge transfer (ICT) character as well as chiral exciton coupling. Strikingly, not only the LUMO, but also the HOMO−1, LUMO+1, and almost all MOs close in energy to the frontier orbitals (Figure S10) reveal through-space electron delocalization. As such, the bands associated with the S2, S9 and S16 excited states relate to strongly mixed transitions within the propeller.

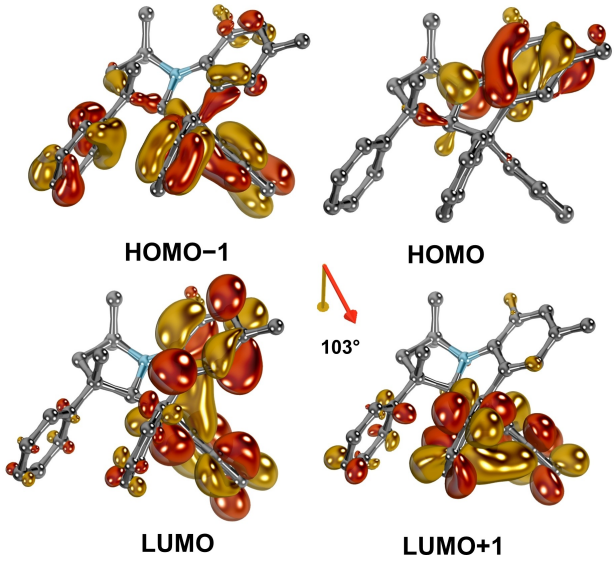

Figure 6. The HOMO−1, LUMO and LUMO+1 suggest chiral exciton coupling. The transition electric dipole moment vector for the transition to the S1 excited state (HOMO→LUMO transition) is given in red, the transition magnetic dipole vector in gold, hydrogen atoms are omitted for clarity.

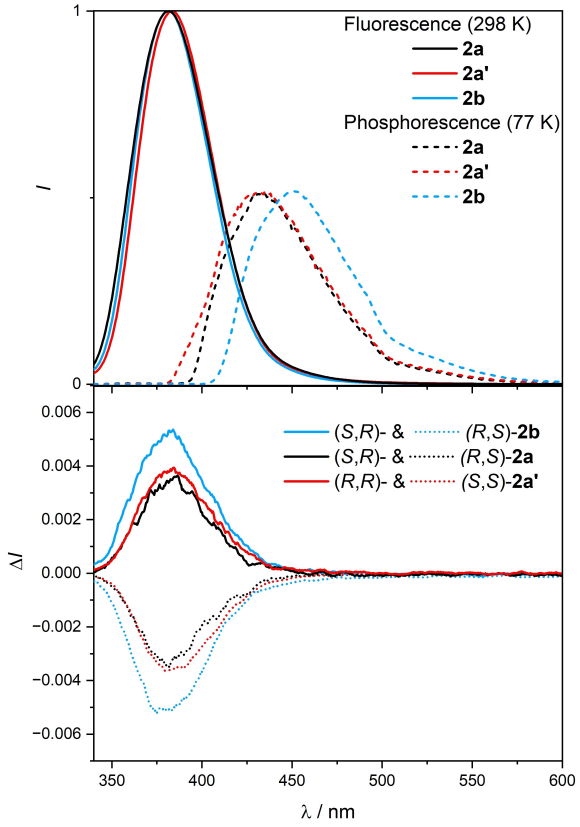

Figure 7. Top: normalized luminescence spectrum of **2b** (blue), **2a** (black) and **2a**′ (red) excited at 330 nm in 2-methyltetrahydrofuran at 298 K (solid lines), with the corresponding phosphorescence emission (dashed lines) recorded using a time-gated mode at 77 K. Bottom: CPL spectra of ***(S,R)***- and ***(R,S)*****-2b** (solid and dotted blue lines, respectively), ***(S,R)***- and ***(R,S)*****-2a** (solid and dotted black lines, respectively) and ***(R,R)***- and ***(S,S)*****-2a**′ (solid and dotted red lines, respectively) measured in toluene (≈10^{-5} M) at 298 K.

An analysis of the relevant electric and magnetic transition dipole moments (μ_e and μ_m, respectively) was performed, along with the dipole and rotatory strength values [Eq. (S1)–(S3)]. The calculated dissymmetry factor of $g_{abs}=8\times10^{-3}$ (S0→S1) is consistent with the experimental value of 1.2×10^{-2}. Computations suggest an angle of $\theta=103°$ between the transition electric- and magnetic dipole moment vectors $\overrightarrow{\mu_e}$ and $\overrightarrow{\mu_m}$ for the S0→S1 transition. This leads to a theoretical rotatory strength of $R=\overrightarrow{\mu_e}\,\overrightarrow{\mu_m}=|\overrightarrow{\mu_e}||\overrightarrow{\mu_e}|\cos(\theta)=98\times10^{-40}$ cgs.

We then turned our attention to the luminescent properties of these chiral compounds, which were very similar for both **2a** and **2b**. As shown in Figure 7, both compounds feature a broad emission profile centered at 380 nm, with Φ of 0.1, and associated fluorescence lifetimes of 4–5 ns (Table S2). Photophysical characterization at low temperature showed an additional emission band at 450 nm for all derivatives. This emission features a characteristic and long decay on the second time-scale (Figure 7 and Table S2), attributed to phosphorescence with an onset at 410 nm, corresponding to T1 energy levels of 3.1 eV. The observation of both fluorescence and phosphorescence within these molecular systems corroborates significant inter-system crossing (ISC) efficiency between the singlet and triplet excited-states. Usually, this occurs only in the presence of heavy atoms such as bromine or iodide (spin orbit coupling), or, if promoted by low-lying n,π* transitions following El-Sayed's rule.[32] The absence of these in **2** suggests that the enhanced ISC results from through-space π-delocalization of electrons within the helical arrangement of the phenyl rings, a feature also observed in helicenes and twisted aromatic derivatives.[33] At room temperature in toluene, these emitters display expected mirror- image CPL spectra with peaks corresponding to those of their respective unpolarized fluorescence emission. The measured g_{lum} values of $+5.3\times10^{-3}$ for ***(S,R)*****-2b** and $+3.5\times10^{-3}$ for ***(S,R)*****-2a** and ***(R,R)*****-2a**′ respectively (Figure 7 and S1), highlight the influence of the enantiopure CAAC scaffold on the overall chirality of the emissive low energy excited state. Note that these values are higher than the ones found for hexa-aryl benzene ($|g_{lum}|=6\times10^{-4}$ at 153 K)[17b] and [2.2]paracyclophane ($|g_{lum}|=1.7\times10^{-3}$ at 298 K)[34] based propellers, which arguably is due to the chiral exciton coupling between the four phenyl rings of both the propeller and the CAAC unit. This mechanism plays a key role in helicene derivatives showing high values of CPL.[35] Finally, the CPL brightness, $\boldsymbol{B}_{CPL}$, of compounds **2b**, **2a** and **2a**′ were estimated to be 0.8, 0.7 and 0.3 $M^{-1}cm^{-1}$, respectively (Table S2).[36] These values are rather modest in comparison to other organic CPL emitters, and reflect the low ε and Φ obtained, suggesting some potential directions for increasing the overall chiroptical properties of these propeller-type chiral CPL emitters.

In conclusion, we have reported the use of cyclic(alkyl)-(amino) carbenes (CAACs) for the preparation of dynamic molecular propellers, which serve as CPL-active emitters.

These helically chiral molecules display through-space electron delocalization and significant intramolecular intersystem crossing (ISC). Detailed spectroscopic and computational investigations indicate residual "sense and report" stereoisomerism of the trityl group to be at the origin of their chiroptical properties. These dynamic systems possess CPL in the blue region at 380 nm with 10 % quantum yield and g_{lum} values as high as 5.3×10^{-3}. We believe that this new class of CPL emitters will establish the use of trityl groups as a structural motif within the family of helically chiral compounds. These results, taken together with the seamless structural variations of CAAC frameworks should be an incentive for the discovery of other purely organic optoelectronic chiral materials derived from carbenes. This topic is currently jointly pursued by this collaborative consortium.

Acknowledgements

The authors acknowledge the Agence Nationale de la Recherche ANR-20-CE07-0000-cResolu (M.M, R.J.), the "prematuration program" of the Centre National de la Recherche scientifique CNRS (J.L.) and the National Science Fundation NSF-CHE-1954380 (G.B.). We also acknowledge the scientific support and HPC resources provided by the Erlangen National High Performance Computing Center (NHR@FAU) of the Friedrich-Alexander-Universität Erlangen-Nürnberg (FAU) under the NHR project n100af and the Deutsche Forschungsgesellschaft (DFG)—440719683 (M.D.). NHR funding is provided by federal and Bavarian state authorities. NHR@FAU hardware is partially funded by the German Research Foundation (DFG)—440719683. This project is cofunded by the European Union (ERC), SHIFUMI, 101041516 (L.F.) and PUSH-IT, 948185 (D.M.). Views and opinions expressed are however those of the author(s) only and do not necessarily reflect those of the European Union or the European Research Council. Neither the European Union nor the granting authority can be held responsible for them. Open Access funding enabled and organized by Projekt DEAL.

Conflict of Interest

The authors declare no conflict of interest.

Data Availability Statement

The data that support the findings of this study are available in the Supporting Information of this article.

Keywords: Carbene · Circularly Polarized Luminescence · Density Functional Theory · Helical · Propeller

[1] a) J. R. Brandt, F. Salerno, M. J. Fuchter, *Nat. Chem. Rev.* **2017**, *1*, 0045; b) J. Crassous, M. J. Fuchter, D. E. Freedman, N. A. Kotov, J. Moon, M. C. Beard, S. Feldmann, *Nat. Rev. Mater.* **2023**, *8*, 365–371.
[2] X. Zhan, F. Xu, Z. Zhou, Y. Yan, J. Yao, Y. S. Zhao, *Adv. Mater.* **2021**, *33*, 2104418.
[3] X. Zhang, J. Yin, J. Yoon, *Chem. Rev.* **2014**, *114*, 4918–4959.
[4] Y. Chen, X. Yang, J. Gao, *Light: Sci. Appl.* **2019**, *8*, 45.
[5] Y.-H. Kim, Y. Zhai, H. Lu, X. Pan, C. Xiao, E. A. Gaulding, S. P. Harvey, J. J. Berry, Z. V. Vardeny, J. M. Luther, M. C. Beard, *Science* **2021**, *371*, 1129–1133.
[6] a) O. Ostroverkhova, *Chem. Rev.* **2016**, *116*, 13279–13412; b) H. Kaji, H. Suzuki, T. Fukushima, K. Shizu, K. Suzuki, S. Kubo, T. Komino, H. Oiwa, F. Suzuki, A. Wakamiya, Y. Murata, C. Adachi, *Nat. Commun.* **2015**, *6*, 8476; c) G. Hong, X. Gan, C. Leonhardt, Z. Zhang, J. Seibert, J. M. Busch, S. Bräse, *Adv. Mater.* **2021**, *33*, 2005630.
[7] Y. L. Gagnon, R. M. Templin, M. J. How, N. J. Marshall, *Curr. Biol.* **2015**, *25*, 3074–3078.
[8] a) Y. Nagata, R. Takeda, M. Suginome, *ACS Cent. Sci.* **2019**, *5*, 1235–1240; b) S. Denmark, *ACS Cent. Sci.* **2019**, *5*, 1117–1119.
[9] a) K. Baek, D. M. Lee, Y. J. Lee, H. Choi, J. Seo, I. Kang, C. J. Yu, J. H. Kim, *Light: Sci. Appl.* **2019**, *8*, 120; b) Y. Deng, M. Wang, Y. Zhuang, S. Liu, W. Huang, Q. Zhao, *Light: Sci. Appl.* **2021**, *10*, 76.
[10] a) L. E. MacKenzie, R. Pal, *Nat. Chem. Rev.* **2020**, *5*, 109–124; b) R. Carr, N. H. Evans, D. Parker, *Chem. Soc. Rev.* **2012**, *41*, 7673–7686.
[11] E. M. Sánchez-Carnerero, A. R. Agarrabeitia, F. Moreno, B. L. Maroto, G. Muller, M. J. Ortiz, S. de la Moya, *Chem. Eur. J.* **2015**, *21*, 13488–13500.
[12] S. Yang, Y. Qu, L. Liao, Z. Jiang, S. Lee, *Adv. Mater.* **2022**, *34*, 2104125.
[13] a) *Helicenes—Synthesis, Properties and Applications*, Wiley-VCH, Weinheim, **2022**; b) J. Crassous, *Circularly Polarized Luminescence of Isolated Small Organic Molecules*, Springer, Singapore, **2020**, pp. 53–97; c) K. Dhbaibi, L. Favereau, J. Crassous, *Chem. Rev.* **2019**, *119*, 8846–8953; d) W.-L. Zhao, M. Li, H.-Y. Lu, C.-F. Chen, *Chem. Commun.* **2019**, *55*, 13793–13803.
[14] a) S. Felder, M.-L. Delcourt, D. Contant, R. Rodríguez, L. Favereau, J. Crassous, L. Micouin, E. Benedetti, *J. Mater. Chem. C* **2023**, *11*, 2053–2062; b) Y. Morisaki, *Circularly Polarized Luminescence of Isolated Small Organic Molecules*, Springer, Singapore, **2020**, pp. 31–52; c) Z. Hassan, E. Spuling, D. M. Knoll, S. Bräse, *Angew. Chem. Int. Ed.* **2020**, *59*, 2156–2170; d) I. Majerz, T. Dziembowska, *J. Phys. Chem. A* **2016**, *120*, 8138–8147; e) H. Hopf, *Modern Cyclophane Chemistry*, Wiley-VCH, Weinheim, **2004**; f) N. Sharma, E. Spuling, C. M. Mattern, W. Li, O. Fuhr, Y. Tsuchiya, C. Adachi, S. Bräse, I. D. W. Samuel, E. Zysman-Colman, *Chem. Sci.* **2019**, *10*, 6689–6696.
[15] a) L. Cui, H. Shinjo, T. Ichiki, K. Deyama, T. Harada, K. Ishibashi, T. Ehara, K. Miyata, K. Onda, Y. Hisaeda, T. Ono, *Angew. Chem. Int. Ed.* **2022**, *61*, e2022043; b) W. Huang, C. Fu, Z. Liang, K. Zhou, Z. He, *Angew. Chem. Int. Ed.* **2022**, *61*, e2022029; c) Y. Imai, *Circularly Polarized Luminescence of Isolated Small Organic Molecules*, Springer, Singapore, **2020**, pp. 11–30; d) S. Hirata, M. Vacha, *J. Phys. Chem. Lett.* **2016**, *7*, 1539–1545.
[16] a) Z. Qiu, C.-W. Ju, L. Frédéric, Y. Hu, D. Schollmeyer, G. Pieters, K. Müllen, A. Narita, *J. Am. Chem. Soc.* **2021**, *143*, 4661–4667; b) Q. Zhou, X. Hou, J. Wang, Y. Ni, W. Fan, Z. Li, X. Wei, K. Li, W. Yuan, Z. Xu, M. Zhu, Y. Zhao, Z. Sun, J. Wu, *Angew. Chem. Int. Ed.* **2023**, e202302266.
[17] a) T. Mori, *Circularly Polarized Luminescence of Isolated Small Organic Molecules*, Springer, Singapore, **2020**, pp. 151–176; b) T. Kosaka, S. Iwai, Y. Inoue, T. Moriuchi, T. Mori, *J. Phys. Chem. A* **2018**, *122*, 7455–7463; c) T. Kosaka, Y. Inoue,

T. Mori, *J. Phys. Chem. Lett.* **2016**, *7*, 783–788; d) D. Gust, A. Patton, *J. Am. Chem. Soc.* **1978**, *100*, 8175–8181.
[18] a) M. Soleilhavoup, G. Bertrand, *Acc. Chem. Res.* **2015**, *48*, 256–266; b) M. Melaimi, R. Jazzar, M. Soleilhavoup, G. Bertrand, *Angew. Chem. Int. Ed.* **2017**, *56*, 10046–10068; c) R. Jazzar, M. Soleilhavoup, G. Bertrand, *Chem. Rev.* **2020**, *120*, 4141–4168.
[19] Selected reviews: a) M. N. Hopkinson, C. Richter, M. Schedler, F. Glorius, *Nature* **2014**, *510*, 485–496; b) U. S. D. Paul, U. Radius, *Eur. J. Inorg. Chem.* **2017**, 3362–3375; c) S. Kundu, S. Sinhababu, V. Chandrasekhar, H. W. Roesky, *Chem. Sci.* **2019**, *10*, 4727–4741; d) R. K. Singh, T. Khan, S. Misra, A. K. Singh, *J. Organomet. Chem.* **2021**, *956*, 122133; e) K. Breitwieser, D. Munz, *Advances in Organometallic Chemistry*, Academic Press, New York, **2022**, pp. 79–132; f) S. Kumar Kushvaha, A. Mishra, H. W. Roesky, K. Chandra Mondal, *Chem. Asian J.* **2022**, *17*, e2021013; g) P. Bellotti, M. Koy, M. N. Hopkinson, F. Glorius, *Nat. Chem. Rev.* **2021**, *5*, 711–725.
[20] a) S. Solé, H. Gornitzka, W. W. Schoeller, D. Bourissou, G. Bertrand, *Science* **2001**, *292*, 1901–1903; b) Z. R. Turner, *Chem. Eur. J.* **2016**, *22*, 11461–11468; c) U. S. D. Paul, U. Radius, *Chem. Eur. J.* **2017**, *23*, 3993–4009; d) C. M. Weinstein, G. P. Junor, D. R. Tolentino, R. Jazzar, M. Melaimi, G. Bertrand, *J. Am. Chem. Soc.* **2018**, *140*, 9255–9260; e) A. E. Samkian, Y. Xu, S. C. Virgil, K.-Y. Yoon, R. H. Grubbs, *Organometallics* **2020**, *39*, 495–499; f) W. Chu, T. Zhou, E. Bisz, B. Dziuk, R. A. Lalancette, R. Szostak, M. Szostak, *Chem. Commun.* **2022**, *58*, 13467–13470.
[21] a) J. Ściebura, P. Skowronek, J. Gawroński, *Angew. Chem. Int. Ed.* **2009**, *48*, 7069–7072; b) B. Stasiak, A. Czapik, M. Kwit, *J. Org. Chem.* **2021**, *86*, 643–656; c) N. Prusinowska, A. Czapik, M. Kwit, *J. Org. Chem.* **2021**, *86*, 6433–6448; d) N. Prusinowska, W. Bendzińska-Berus, M. Jelecki, U. Rychlewska, M. Kwit, *Eur. J. Org. Chem.* **2015**, 738–749; e) A. Janiak, J. Ściebura, W. Bendzińska-Berus, J. Grajewski, U. Rychlewska, J. Gawroński, *Tetrahedron: Asymmetry* **2016**, *27*, 811–814.
[22] a) D. Pichon, M. Soleilhavoup, J. Morvan, G. P. Junor, T. Vives, C. Crévisy, V. Lavallo, J. M. Campagne, M. Mauduit, R. Jazzar, G. Bertrand, *Chem. Sci.* **2019**, *10*, 7807–7811; b) J. Morvan, F. Vermersch, Z. Zhang, L. Falivene, T. Vives, V. Dorcet, T. Roisnel, C. Crévisy, L. Cavallo, N. Vanthuyne, G. Bertrand, R. Jazzar, M. Mauduit, *J. Am. Chem. Soc.* **2020**, *142*, 19895–19901; c) A. Madron du Vigné, N. Cramer, *Organometallics* **2022**, *41*, 2731–2741.
[23] F. Vermersch, L. Oliveira, J. Hunter, M. Soleilhavoup, R. Jazzar, G. Bertrand, *J. Org. Chem.* **2022**, *87*, 3511–3518.
[24] N. Berova, L. Di Bari, G. Pescitelli, *Chem. Soc. Rev.* **2007**, *36*, 914–931.
[25] a) J. Ściebura, J. Gawroński, *Tetrahedron: Asymmetry* **2013**, *24*, 683–688; b) L. Wang, T. Zhang, B. K. Redden, C. I. Sheppard, R. W. Clark, M. D. Smith, S. L. Wiskur, *J. Org. Chem.* **2016**, *81*, 8187–8193; c) M. Kemper, E. Engelage, C. Merten, *Angew. Chem. Int. Ed.* **2021**, *60*, 2958–2962; d) M. Kemper, S. Reese, E. Engelage, C. Merten, *Chem. Eur. J.* **2022**, *28*, e2022028.
[26] Deposition Numbers 2252188 (for **(*R*,*S*)-2a**) and 2252189 (for **(*S*,*R*)-2b**) contain the supplementary crystallographic data for this paper. These data are provided free of charge by the joint Cambridge Crystallographic Data Centre and Fachinformationszentrum Karlsruhe Access Structures service.
[27] a) F. Neese, F. Wennmohs, U. Becker, C. Riplinger, *J. Chem. Phys.* **2020**, *152*, 224108; b) S. Grimme, A. Hansen, S. Ehlert, J. M. Mewes, *J. Chem. Phys.* **2021**, *154*, 064103; c) C. Riplinger, F. Neese, *J. Chem. Phys.* **2013**, *138*, 034106; d) C. Riplinger, B. Sandhoefer, A. Hansen, F. Neese, *J. Chem. Phys.* **2013**, *139*, 134101.
[28] a) J. D. Andose, K. Mislow, *J. Am. Chem. Soc.* **1974**, *96*, 2168–2176; b) M. R. Kates, J. D. Andose, P. Finocchiaro, D. Gust, K. Mislow, *J. Am. Chem. Soc.* **1975**, *97*, 1772–1778; c) J. P. Hummel, E. P. Zurbach, E. N. DiCarlo, K. Mislow, *J. Am. Chem. Soc.* **1976**, *98*, 7480–7483.
[29] J. Ściebura, J. Gawroński, *Chem. Eur. J.* **2011**, *17*, 13138–13141.
[30] K. Dhbaibi, L. Abella, S. Meunier-Della-Gatta, T. Roisnel, N. Vanthuyne, B. Jamoussi, G. Pieters, B. Racine, E. Quesnel, J. Autschbach, J. Crassous, L. Favereau, *Chem. Sci.* **2021**, *12*, 5522–5533.
[31] a) M. de Wergifosse, J. Seibert, S. Grimme, *J. Chem. Phys.* **2020**, *153*, 084116; b) C. Bannwarth, S. Grimme, *Comput. Theor. Chem.* **2014**, *1040–1041*, 45–53.
[32] a) S. K. Lower, M. A. El-Sayed, *Chem. Rev.* **1966**, *66*, 199–241; b) Z. An, C. Zheng, Y. Tao, R. Chen, H. Shi, T. Chen, Z. Wang, H. Li, R. Deng, X. Liu, W. Huang, *Nat. Mater.* **2015**, *14*, 685–690; c) S. Hirata, *Adv. Opt. Mater.* **2017**, *5*, 1700116; d) H. Ma, Q. Peng, Z. An, W. Huang, Z. Shuai, *J. Am. Chem. Soc.* **2019**, *141*, 1010–1015.
[33] a) K. Nagarajan, A. R. Mallia, K. Muraleedharan, M. Hariharan, *Chem. Sci.* **2017**, *8*, 1776–1782; b) N. I. Nijegorodov, W. S. Downey, *J. Phys. Chem.* **1994**, *98*, 5639–5643; c) Y. Xu, Q. Wang, X. Song, Y. Wang, C. Li, *Chem. Eur. J.* **2023**, *29*, e2022034.
[34] G. Namba, Y. Mimura, Y. Imai, R. Inoue, Y. Morisaki, *Chem. Eur. J.* **2020**, *26*, 14871–14877.
[35] K. Dhbaibi, L. Favereau, M. Srebro-Hooper, M. Jean, N. Vanthuyne, F. Zinna, B. Jamoussi, L. Di Bari, J. Autschbach, J. Crassous, *Chem. Sci.* **2018**, *9*, 735–742.
[36] L. Arrico, L. Di Bari, F. Zinna, *Chem. Eur. J.* **2021**, *27*, 2920–2934.

Manuscript received: April 17, 2023
Accepted manuscript online: May 23, 2023
Version of record online: July 10, 2023